through recrystallization, probably in response to the combined influence of high temperatures ($\gtrsim -10$°C) and high strain rates (*13*); fluctuations in magnitude or orientation of stresses also may help form this fabric (*25*). High strain rates and fluctuating stresses characterize the base of the Greenland ice sheet at Camp Century and Dye 3, but temperatures are less than −13°C and a single-maximum fabric is developed (*16–18, 24, 26*). Recrystallization under strong basal shear thus seems to require high temperatures. The importance of fluctuating stresses is still uncertain.

A multiple-maximum recrystallization fabric is developed on ice shelves (*11, 27*); *c*-axis concentrations are greater than 10% per 1% area at temperatures less than −20°C at shallow depth, and concentrations strengthen with increasing temperature and strain at greater depth (*27*). Ice shelves are dominated by normal stresses, and strain rates are greater than $\sim 10^{-3}$ year^{-1}. Comparison to inland regions shows that strain rates must be greater than $\sim 10^{-3}$ year^{-1} to cause rapid recrystallization under normal stresses at temperatures less than ~−10°C, but that strain rates greater than $\sim 10^{-1}$ year^{-1} and temperatures greater than ~−10°C are necessary for recrystallization under simple shear.

The textures, temperatures, and strain rates in ice shelves with multiple-maximum fabrics are similar to those at the UpB camp on ice stream B, Antarctica (*28, 29*). This suggests that recrystallization also dominates at UpB. Strain at UpB is longitudinally extensional and vertically and transversely compressional (*29*); therefore, my model predicts that a fabric similar to that of Fig. 1D but with local concentrations arising from recrystallization should occur. Preliminary seismic results from ice stream B indicate that *c* axes do cluster near a transverse vertical plane (*30*), as predicted.

A complex strain history commonly leads to a complex fabric. Strains in excess of 100% may be required to remove evidence of a previous fabric by way of grain rotation; however, recrystallization will reduce the strain that is needed to generate a new fabric (*2*).

REFERENCES AND NOTES

1. P. V. Hobbs, *Ice Physics* (Clarendon, Oxford, 1974), pp. 274–280.
2. P. Duval *et al.*, *J. Phys. Chem.* **87**, 4066 (1983).
3. N. Azuma and A. Higashi, *Ann. Glaciol.* **6**, 130 (1985).
4. In an incompressible plastic such as ice, uniaxial compression has $\varepsilon_2 = \varepsilon_3 = -\varepsilon_1/2$, where ε_i are the principal stress deviators, $\varepsilon_1 < 0$ is compressive, and $\varepsilon_3 > 0$ is extensional. Uniaxial tension has $\varepsilon_1 = \varepsilon_2 = -\varepsilon_3/2$, and pure shear has $\varepsilon_1 = -\varepsilon_3$, $\varepsilon_2 = 0$.
5. S. Fujita, M. Nakawo, S. Mae, *Proc. Natl. Inst. Polar Res. (Jpn) No. 1* (1987), p. 122.
6. P. Pimienta, P. Duval, V. Ya. Lipenkov, *Int. Assoc. Hydrological Sci. Publ. 170* (1987), pp. 57–66.
7. Stresses that do not cause rigid-body rotations are "normal" or "irrotational" stresses.
8. Growth selection, the growth of grains that are favorably oriented in the stress field at the expense of other grains, may be important in some cases but generally produces fabrics similar to those provided by recrystallization.
9. A. J. Gow and T. Williamson, *U.S. Army Corps Eng. Cold Reg. Res. Eng. Lab. Rep. 76-35* (1976), pp. 1–25.
10. M. Matsuda and G. Wakahama, *J. Glaciol.* **21**, 607 (1978).
11. W. F. Budd, *Z. Gletscherk. Glazialgeol.* **8**, 65 (1972).
12. B. Kamb, in *Flow and Fracture of Rocks, Geophysical Monograph 16,* N. C. Heard, I. Y. Borg, N. C. Carter, C. B. Raleigh, Eds. (American Geophysical Union, Washington, DC, 1972), pp. 211–241.
13. R. L. Hooke and P. J. Hudleston, *J. Glaciol.* **25**, 195 (1980).
14. R. W. Cahn, in *Physical Metallurgy,* R. W. Cahn and P. Haasen, Eds. (North-Holland, Amsterdam, ed. 3, 1983), part II, pp. 1595–1671.
15. D. D. Blankenship and C. R. Bentley, *Int. Assoc. Hydrological Sci. Publ. 170* (1987), pp. 17–28.
16. S. L. Herron and C. C. Langway, Jr., *Ann. Glaciol.* **3**, 118 (1983).
17. K. Taylor, thesis, University of Wisconsin–Madison (1982).
18. S. L. Herron *et al.*, in *Greenland Ice Core: Geophysics, Geochemistry, and the Environment, Geophysical Monograph 33,* C. C. Langway, H. Oeschger, W. Dansgaard, Eds. (American Geophysical Union, Washington, DC, 1985), pp. 23–31.
19. D. J. Drewry, Ed., *Antarctica: Glaciological and Geophysical Folio* (Scott Polar Research Institute, Cambridge, 1983); I. M. Whillans and S. J. Johnsen, *J. Glaciol.* **29**, 78 (1983); W. F. Budd and N. W. Young, in *The Climatic Record in Polar Ice Sheets,* G. de Q. Robin, Ed. (Cambridge Univ. Press, Cambridge, 1983), pp. 150–177; I. M. Whillans *et al.*, *Ann. Glaciol.* **5**, 185 (1984).
20. The statistical significance of this ellipticity is uncertain (*13*), and its orientation relative to the stress axes has not been measured directly because azimuthally oriented cores were not collected.
21. Alternatively, the stress state may limit grain-boundary motion to narrow zones between grains; therefore, grain growth stops because no grains are consumed by neighbors [P. Pimienta and P. Duval, *J. Phys.* **48**, Colloque C1, 243 (1987)]. If this happens, then recrystallization, which would decrease grain sizes, does not occur.
22. P. Pimienta, P. Duval, V. Ya. Lipenkov, A. N. Salamatin, *Ann. Glaciol.* **10**, 137 (1988).
23. R. Naruse and H. Shimizu, *Mem. Natl. Inst. Polar Res. (Jpn), Spec. Issue 7* (1978), p. 227. The flow just at Mizuho shows vertical extension because of local topography (Y. Abe, A. Yoshimura, R. Naruse, *ibid.*, p. 37), but flow lines and thickness patterns suggest approximately longitudinal uniaxial extension along most of the flow line leading to Mizuho; O. N. Vinogradov, *Trans. Soviet Antarct. Exped.* **60**, 100 (1972).
24. D. Dahl-Jensen and N. S. Gundestrup, *Int. Assoc. Hydrological Sci. Publ. 170* (1987), pp. 31–43.
25. N. W. Young *et al.*, *Aust. Natl. Antarct. Res. Exped. Res. Notes 28* (1985), pp. 18–24.
26. G. de Q. Robin, in *The Climatic Record in Polar Ice Sheets,* G. de Q. Robin, Ed. (Cambridge Univ. Press, Cambridge, 1983), pp. 94–97.
27. A. J. Gow, *U.S. Army Corps Eng. Cold Reg. Res. Eng. Lab. Res. Rep. 282* (1970), pp. 1–20.
28. R. B. Alley and C. R. Bentley, *Ann. Glaciol.*, in press.
29. I. M. Whillans, personal communication.
30. D. D. Blankenship and C. R. Bentley, *Ann. Glaciol.*, in press.
31. C. C. Langway, Jr., *U.S. Army Snow, Ice, Permafrost Res. Est. Tech. Rep. 62* (1958), pp. 1–16.
32. The natural octahedral unit shear, $\bar{\gamma}_o$, is given by $\bar{\gamma}_o = (2/3)[(\varepsilon_1 - \varepsilon_2)^2 + (\varepsilon_2 - \varepsilon_3)^2 + (\varepsilon_3 - \varepsilon_1)^2]^{1/2}$ where ε_j are the principal strains (*13*).

33. I thank C. R. Bentley, D. D. Blankenship, S. T. Rooney, and an anonymous reviewer for helpful suggestions and A. N. Mares and S. H. Smith for manuscript and figure preparation. Supported by the NSF Division of Polar Programs. This is contribution number 493 of the Geophysical and Polar Research Center, University of Wisconsin–Madison.

9 December 1987; accepted 24 February 1988

Superconducting and Magnetic Behavior in $La_{2-x}Na_xCuO_4$

M. A. SUBRAMANIAN, J. GOPALAKRISHNAN, C. C. TORARDI, T. R. ASKEW, R. B. FLIPPEN, A. W. SLEIGHT, J. J. LIN, S. J. POON

New phases of the type $La_{2-x}A^{1+}_xCuO_{4-y}$ have been prepared where A^{1+} is sodium or potassium. The sodium phases are superconducting for x values from 0.2 to 0.5 at temperatures up to about 40 K. In addition, there are unusual magnetic properties below about 10 K that may be indicative of spin glass behavior. Phases of the type $La_{2-x}K_xCuO_{4-y}$ could only be prepared with x values up to about 0.1, and these phases are not superconducting above 4.2 K.

FOLLOWING THE DISCOVERY OF high-temperature superconductivity in the La-Ba-Cu-O system by Bednorz and Müller (*1*), it has been shown that alkaline-earth metal substitution in La_2CuO_4, $La_{2-x}A_xCuO_4$ where A is calcium, strontium, or barium, gives rise to superconductivity in this system in the 20 to 40 K range (*2*). One of us (*3*) has argued that superconductivity in this system is closely related to the strong electropositive character of A atoms that can stabilize Cu^{III} and render the Cu–O bonds more covalent. This hypothesis is further strengthened by the observation that substitution of Pb^{II} and Cd^{II} in La_2CuO_4 does not give rise to superconductivity (*4*). Accordingly, we have studied the substitution of strongly electropositive alkali metal cations into La_2CuO_4. Prior attempts (*5*) to substitute potassium in

M. A. Subramanian, J. Gopalakrishnan, C. C. Torardi, T. R. Askew, R. B. Flippen, A. W. Sleight, Central Research and Development Department, E. I. du Pont de Nemours and Company, Experimental Station, Wilmington, DE 19898.
J. J. Lin and S. J. Poon, Department of Physics, University of Virginia, Charlottesville, VA 22906.

La_2CuO_4 have not been successful. We have been able to substitute both sodium and potassium into La_2CuO_4 giving rise to the $La_{2-x}A^{1+}_xCuO_4$ (A = Na and K) series; of these, only the sodium-substituted samples exhibit superconductivity above 4.2 K. We report here the synthesis, structure, superconductivity (up to about 40 K), and unusual magnetic properties of this new series of oxides.

Members of the $La_{2-x}Na_xCuO_4$ series for various values of x up to $x = 0.5$ were prepared. Stoichiometric amounts of La_2O_3, CuO, and Na_2O_2 were mixed and loaded into gold tubes inside a dry box, and the ends of the tubes were closed by welding.

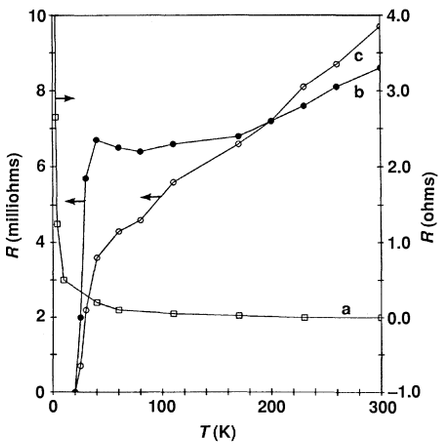

Fig. 1. Resistivity curves for $La_{2-x}Na_xCuO_{4-y}$ samples. Curve a: $x = 0.1$; curve b: $x = 0.3$; and curve c: $x = 0.5$. The room temperature–specific resistivities of these samples are 11.1, 2.8, and 2.2 milliohm-cm, respectively.

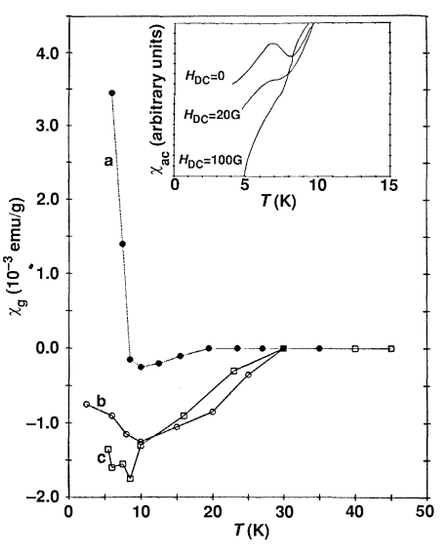

Fig. 2. Magnetic susceptibility χ_g for $La_{2-x}Na_xCuO_{4-y}$ samples. Curve a: $x = 0.5$, prepared at atmospheric conditions; curve b: $x = 0.3$, prepared under 3 kbar; and curve c: $x = 0.5$, prepared under 3 kbar. Inset shows magnetic susceptibility data at different fields H_{DC} for $x = 0.5$ samples prepared under 3 kbar.

The sealed gold tubes were heated at 800° to 900°C for 24 to 36 hours in air. Alternatively, gold tubes with the same starting mixtures were heated to 850° to 900°C for 24 hours under an external pressure of 3 kbar. For $La_{2-x}K_xCuO_4$ samples, KO_2 was used as the source of potassium. Total copper content was determined by iodometric titration, and Cu^{III} content was determined by reaction with a standard Fe^{II} solution (*6*). The results (Table 1) show that samples prepared at 3 kbar O_2 pressure in sealed gold tubes contain larger concentrations of Cu^{III}.

Powder x-ray diffraction patterns were obtained on all products with a SCINTAG diffractometer by using CuK_α radiation, and the unit cell edges (Table 2) were refined by a least-squares fit. As for the $La_{2-x}A^{2+}_xCuO_4$ series where A is calcium, strontium, or barium, the room temperature symmetry changes from orthorhombic to tetragonal with increasing values of x. Also, the a cell edge distance decreases with increasing values of x. The Cu–O distance is one-half that of the a edge; thus, for the $La_{2-x}Na_xCuO_4$ series, the Cu–O distance decreases from 1.901 ± 0.002 Å at $x = 0.0$ to 1.888 ± 0.002 Å for $x = 0.3$.

Structural refinements based on neutron diffraction data taken from polycrystalline samples were performed for $La_{1.8}Na_{0.2}CuO_4$, $La_{1.7}Na_{0.3}CuO_4$, and $La_{1.8}K_{0.2}CuO_4$ at room temperature and for $La_{1.8}Na_{0.2}CuO_4$ at 10 K. These data were collected at Brookhaven National Laboratory and were refined by the Rietveld profile analysis method (*7*). The neutron scattering powers of lanthanum (0.827), sodium (0.363), and potassium (0.367) are such that these refinements do not lead to an accurate assessment of the alkali content of these phases. The room temperature data for $La_{1.8}Na_{0.2}CuO_4$ and $La_{1.7}Na_{0.3}CuO_4$ readily refined in the tetragonal space group *I4/mmm*, as in the case of the $La_{2-x}A^{2+}_xCuO_4$ phases. The $La_{1.8}K_{0.2}CuO_4$ room temperature data and the $La_{1.8}Na_{0.2}CuO_4$ data taken at 10 K indicate orthorhombic symmetry but with a distortion from tetragonal that is much less than in the case of pure La_2CuO_4. Agreement factors (R_{wp}) in the range from 7.5 to 8.0 were obtained; details will be reported elsewhere (*8*).

The resistance R as a function of temperature was measured with a four-terminal technique (Fig. 1). The $x = 0.1$ sample shows a small negative temperature coefficient of resistance above 40 K; it exhibits semiconducting behavior, with resistivity increasing rapidly as temperatures is lowered. However, both the $x = 0.3$ and 0.5 samples show metal-like resistance behavior. Below ~40 K, R drops more rapidly and an apparent zero resistance (10^{-9} ohms) is achieved at 20 K. To confirm the superconducting state in these samples, Meissner effect (flux exclusion) measurements were performed. Magnetization was measured by use of a SQUID susceptometer as the samples were cooled from 50 to 7 K in an applied field of 20 Oe. The $x = 0.3$ and 0.5 samples showed a diamagnetic signal corresponding to ≈10% of that estimated for a complete Meissner effect, indicative of bulk superconductivity. To further characterize the magnetic state at low temperature, magnetic studies were performed on samples prepared at different pressures. Figure 2 shows results on the $x = 0.5$ samples. The diamagnetic signals from the sample prepared at 3-kbar pressure are about an order of magnitude larger than the ones prepared at atmospheric pressure. Below 10 K, both samples show a susceptibility maximum at 7 K in an ac measurement (Fig. 2). These susceptibility maxima were suppressed in moderate dc fields of 20 to 100 Oe, characteristic of that observed in spin glasses. High-temperature susceptibility measurement on both samples yielded similar effective moments of ~0.43 μ_B per copper atom. However, samples prepared at low pressure show a positive Curie-Weiss intercept (~+10 K) indicating ferromagnetic interactions, whereas the samples prepared at high pressure show a negative intercept (~−16 K) indicative of antiferromagnetic interactions. This is con-

Table 1. Concentration of Cu^{III} in samples of $La_{2-x}Na_xCuO_{4-y}$.

Nominal composition	Pressure	Cu^{III}/total Cu	y*
$La_{1.8}Na_{0.2}CuO_{4-y}$	1 atm	0.15	0.12
$La_{1.8}Na_{0.2}CuO_{4-y}$	3 kbar	0.19	0.11
$La_{1.7}Na_{0.3}CuO_{4-y}$	1 atm	0.18	0.21
$La_{1.7}Na_{0.3}CuO_{4-y}$	3 kbar	0.21	0.20

*The values of y were calculated for the data in column 3 by assuming the nominal composition given in column 1.

Table 2. Cell dimensions for some $La_{2-x}A^{+}_xCuO_4$ oxides at room temperature. La_2CuO_4 is actually orthorhombic; the "a" value is $(a+b)/2\sqrt{2}$. The numbers in parentheses are the standard errors of the mean expressed as deviations in the last digit reported.

Nominal composition	a (Å)	c (Å)
La_2CuO_4	3.802(2)	13.167(4)
$La_{1.9}Na_{0.1}CuO_4$	3.783(3)	13.179(6)
$La_{1.8}Na_{0.2}CuO_4$	3.778(2)	13.176(5)
$La_{1.7}Na_{0.3}CuO_4$	3.775(3)	13.170(5)
$La_{1.5}Na_{0.5}CuO_4$	3.775(4)	13.156(9)
$La_{1.8}K_{0.2}CuO_4$*	3.783(3)	13.192(8)

*Values given are for pseudotetragonal cell from powder x-ray data. Neutron diffraction data reveals orthorhombic symmetry with $a = 5.3596(3)$, $b = 5.3431(2)$, and $c = 13.1933(6)$ Å.

sistent with the large paramagnetic signals observed in the diamagnetic regime in samples prepared at low pressure.

During our concurrent investigation of the Na-Cu-O system, we have discovered a phase that becomes ferromagnetic at ~10 K. Thus, we carefully considered the possibility that an impurity of this phase could cause the unusual magnetic behavior of $La_{2-x}Na_xCuO_4$ samples at ~10 K. However, the observed moments at low temperature for our samples prepared at low pressure are such that the amount of ferromagnetic impurity would have to exceed by several times the amount of the host material, and our x-ray diffraction patterns show essentially single-phase $La_{2-x}Na_xCuO_4$. Thus we have concluded that the unusual magnetic behavior observed in $La_{2-x}Na_xCuO_4$ is not due to a ferromagnetic impurity.

It is possible to produce superconductivity in the La-Cu-O system by purposely preparing a phase off the ideal La_2CuO_4 stoichiometry (*9*). However, under our conditions of synthesis, we observe no superconductivity above 4.2 K for $La_{2-x}A^{1+}_xCuO_4$ phases over the range of x from 0.0 to 0.1. The substitution of the alkali cation sodium for lanthanum apparently must exceed 5% before metallic and superconducting properties occur. Assuming no oxygen deficiency or peroxide formation, we would express the oxidation states as $La^{III}_{2-x}Na^{I}_xCu^{II}_{1-2x}Cu^{III}_{2x}O_4$. The measured Cu^{III} concentration (Table 1) is always less than this formula predicts thus indicating that there is always some oxygen deficiency. However, the amount of oxygen deficiency may be decreased by using high oxygen pressure. The present results indicate that oxygen deficiency is a key factor in determining the sign of the magnetic interaction and thus the nature of the magnetic ground state. Lower oxygen deficiency improves the superconducting properties and also accentuates the lower temperature magnetic behavior that may be indicative of the coexistence of spin glass and superconductivity in these novel materials.

REFERENCES AND NOTES

1. J. G. Bednorz and K. A. Müller, *Z. Phys. B* **64**, 189 (1986).
2. See, for example, K. Fueki *et al. ACS Symp. Ser.* **351**, 38 (1987).
3. A. W. Sleight, *ibid.*, p. 2.
4. J. Gopalakrishnan *et al.*, *J. Solid State Chem.*, in press.
5. S. M. Fine *et al.*, *ACS Symp. Ser.* **351**, 95 (1987).
6. M. W. Shafer, T. Penney, B. L. Olson, *Phys. Rev. B* **36**, 4047 (1987).
7. H. M. Rietveld, *J. Appl. Crystallogr.* **2**, 65 (1969).
8. C. C. Torardi *et al.*, in preparation.
9. P. M. Grant *et al.*, *Phys. Rev. Lett.* **58**, 2482 (1987).
10. We thank P. M. Kelly and C. R. Walther for their technical assistance.

22 February 1988; accepted 21 March 1988

Subsidence in the Northeastern Nile Delta: Rapid Rates, Possible Causes, and Consequences

DANIEL JEAN STANLEY

Holocene fluvial and marine deposits have accumulated in a graben-like structure on the northeastern margin of the Nile delta. This part of the delta, which includes Lake Manzala, Port Said, and the northern Suez Canal, has subsided rapidly at rates of up to 0.5 centimeter per year since about 7500 years ago. This subsidence has diverted at least four major distributaries of the Nile River into this region. The combined effects of continued subsidence and sea level rise may flood a large part of the northern delta plain by as much as 1 meter by the year 2100. The impact of continued subsidence, now occurring when sediment input along the coast has been sharply reduced because of the Aswan High Dam, is likely to be substantial, particularly in the Port Said area and as far inland as south of Lake Manzala.

THE CONFIGURATION OF THE NILE delta in Egypt, the major depocenter in the eastern Mediterranean, has changed markedly during the Holocene and continues to evolve rapidly (*1*). Geologic evolution of the northern delta plain margin has been controlled largely by interplay of eustatic sea level fluctuations (*2*), climatic variations (*3*), which affect Nile River flow and sediment discharge (*4*), the erosional effects of eastward-directed coastal and nearshore Mediterranean currents (*5*), man's activity since pre-Dynastic time (*6*), and neotectonics. The migration of the distributary channels of the Nile River through time (*7*) has affected the morphology of the delta and the general subsurface distribution of upper Quaternary sediment facies (*8*, *9*). Recent workers have investigated the stratigraphy, petrology, and radiocarbon age of numerous drill-core sections. Studies of these cores provide a chronostratigraphic base with which to interpret more precisely recent changes that have affected this delta. These cores have been used to determine the uppermost Pleistocene through Holocene shifts of coastlines and delta lobes on the northeastern delta margin (*2*) and to show that the shoreline in the northeastern delta prograded northward by as much as 50 km during the past 5000 years (an average rate of about 10 m/year).

Mediterranean Basin Project, U.S. National Museum of Natural History, Smithsonian Institution, Washington, DC 20560.

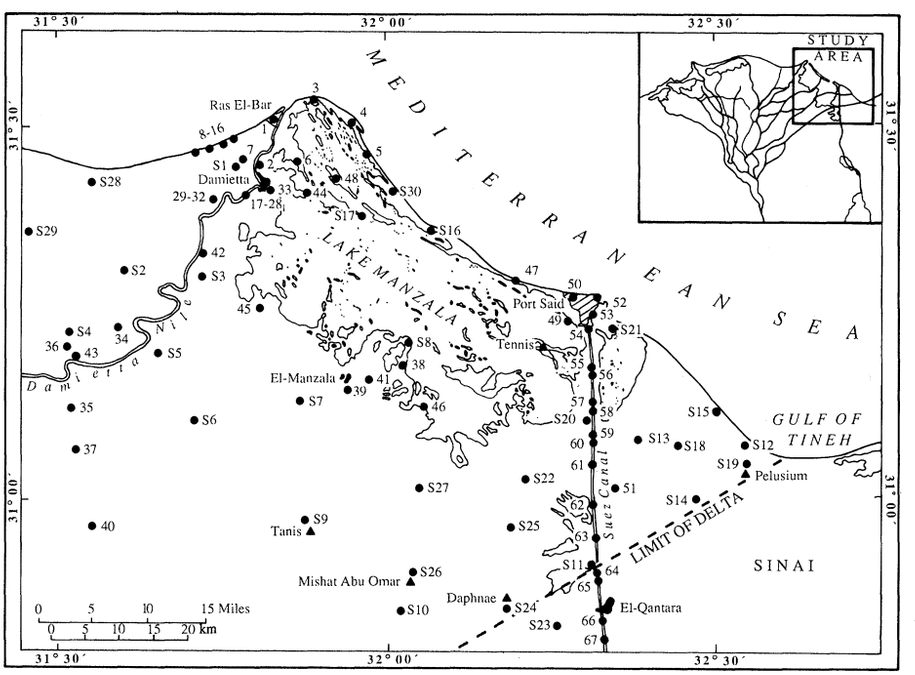

Fig. 1. Map of the northeastern Nile delta that shows the location of Smithsonian cores (S-1 to S-30, Table 1) and other borings (1 to 67, Table 2). Former major Nile River distributaries (4 in study area) are shown in inset.